Depolarization effects due to the interaction between adsorbed dipoles on stepped surfaces

E. V. Albano*
Instituto de Investigaciones Fisicoquímicas Teóricas y Aplicadas, Facultad de Ciencias Exactas–Universidad Nacional de La Plata, Casilla de Correo 16, Sucursal 4-(1900) La Plata, Argentina

H. O. Mártin
Departamento de Física, Facultad de Ciencias Exactas, Universidad Nacional de La Plata, Casilla de Correo 67, (1900) La Plata, Argentina

(Received 10 February 1988)

A generalization of the Helmholtz equation for the interpretation of adsorbate-induced work-function changes (WFC's) on stepped surfaces, which accounts for mutual depolarization effects on the adlayer, is studied and discussed. The proposed equation, in connection with concentration profiles obtained through Monte Carlo simulations, allows us to study simultaneously depolarization and adsorbate distribution effects on the WFC. The limitations of WFC versus coverage measurements, performed at constant temperature on stepped and polycrystalline substrata, to obtain information about the surface distribution and the polarizability of the adsorbate are also discussed. The dependence of the electrical depolarization fields and the dipolar interaction energy on both the polarizability and the distance to the step have also been studied. It is found that under certain circumstances specified in the text, the model predicts an unexpected phenomenon called depolarization-induced dipole inversion, consisting in the change of the direction of some dipoles due to the dipolar interaction. This phenomenon would cause an oscillatory behavior of the curves of WFC versus coverage, provided that the nucleation of the adsorbate at the steps proceeds in a row-by-row mode.

I. INTRODUCTION

Experimental evidence of dipolar interaction between adsorbed particles on single crystals has been widely reported. Typical examples arise from measurements of adsorbate-induced work-function changes (henceforth WFC's),[1–5] thermal-desorption traces (henceforth TD),[3–6] and high-resolution ir spectroscopy (henceforth HRIRS),[7,8] etc. Also, models based on the calculation of the depolarization effects and energetic interactions for a planar array of adparticles, considered as point dipoles, have contributed to the understanding of the above-mentioned experiments (see, for example, Refs. 1 and 9–12 for WFC's, Ref. 13 for TD, and Refs. 7 and 8 for HRIRS).

Directing our attention to the interpretation of WFC's ($\Delta\phi$), the original description is based on the well-known Helmholtz equation,[1] derived from classical electrostatics for a continuous dipole sheet, which may be written as

$$\Delta\theta = -4\pi N p \ , \tag{1}$$

where N is the number of adparticles per unit surface area and p is the corresponding dipole moment. More refined models have since been developed in order to correlate the measured WFC with the microscopic properties of the respective system.[1,9–12,14]

The aim of this work is first to generalize Eq. (1) in order to interpret WFC's on stepped surfaces, considering both depolarization effects between the adsorbed dipoles and the substantial difference, frequently reported, between the dipole moment of adparticles at step sites and on terrace sites (see, for example, the recompilation of available experimental data in Ref. 15). Secondly, the model proposed here, in connection with concentration profiles derived through Monte Carlo simulations, is employed to study the influence of the polarizability, the temperature, and the adatom-adatom and adatom-step interactions on the WFC's. Interest in the present work also arises because atoms at step sites contribute most to the concentration of surface defects in crystalline substrata.[16] The study also gives insight into the understanding of WFC's on polycrystalline samples. The structure of the work is the following. The proposed generalization of Eq. (1) is derived in Sec. II. The Monte Carlo procedure used to evaluate the concentration profiles is briefly reviewed in Sec. III. The results are presented and discussed in Sec. IV and the conclusions are stated in Sec. V.

II. THEORY

In order to evaluate the modifications which have been introduced in the Helmholtz equation [Eq. (1)] to account for depolarization effects between adsorbed dipoles on stepped-metal surfaces, let us consider that the dipoles are adsorbed on a square lattice of size $L \times L_T$, where L and L_T (with $L \gg L_T$) are the terrace length (which is parallel to the step) and the terrace width, respectively. In the present work it is assumed that the dipole moment of the adparticles is positive (negative) when it is pointing away from (toward) the surface, causing the work func-

tion to decrease (increase). Only the component of the dipole moment perpendicular to the surface, which is the relevant one for the evaluation of the WFC's, will be considered. The interaction between dipoles adsorbed on different terraces is neglected. This approximation is reasonable at low coverage and temperature due to the preferential nucleation of particles close to the steps.[15] Furthermore, the error due to this assumption decreases when increasing the terrace width.

Let us direct our attention to a typical dipole adsorbed on a site of coordinates (i,j) of the square lattice, with $1 \leq i \leq L_T$ and $-L/2 \leq j \leq L/2$. The indices i and j refer to rows parallel to and columns perpendicular to the step, respectively. In order to avoid boundary effects, the calculations will be performed in the limit $L = \infty$; therefore it is convenient to select the typical dipole at the column $j=0$ taking advantage of the symmetry without loss of generality. Let p_{ij}^0 be the component normal to the surface of the dipole moment of an isolated particle adsorbed at the site (i,j). When the coverage increases, p_{ij}^0 changes into p_{ij} due to the depolarization effects, that is,

$$p_{ij} = p_{ij}^0 + \alpha E_{ij} \ , \tag{2}$$

where α is the polarizability of the adparticles and E_{ij} is the depolarization electrical field acting on the position of the considered dipole, which is given by

$$E_{ij} = E_{ij}^1 + E_{ij}^2 \ . \tag{3}$$

The depolarization fields E_{ij}^n $(n=1,2)$ are due to adsorbed dipoles $(n=1)$ and their respective images $(n=2)$.

The physical origin of the dipole moment of an isolated adsorbed particle merits a brief comment. The surface of a clean metal has an extremely inhomogeneous short-range electrical field[9] which induces the polarization of the adsorbate. The component normal to the surface of the permanent dipole of the particle in the gas phase (if it has any), self-depolarization, and charge-transfer effects also contribute to the dipole moment of the adsorbed particle. To make the problem more tractable, all the above-mentioned effects are assumed to be included in the parameter p_{ij}^0, independent of the surface coverage. p_{ij}^0 can be experimentally determined from the slope at the low-coverage regime of WFC versus coverage curves [see Eq. (1) and the discussion below].

For the evaluation of the electrical depolarization fields it is reasonable to assume that on the average, the dipole moments of the particles adsorbed at the same distance from the step are of the same magnitude. Consequently, the same argument is valid for the electrical fields and therefore one can leave aside the index j in Eqs. (2) and (3). According to the classical electrostatics, E_i^1 is given by

$$E_i^1 = -\sum_{k=1}^{L_T} \sum_{l=-L/2}^{L/2} p_{kl} a^{-3} [(k-i)^2 + l^2]^{-3/2} \tag{4}$$

with the restriction $(k,l) \neq (i,0)$, where a is the nearest-neighbor distance on the square lattice. Under the assumption just mentioned, one has that

$$p_{kl} = p_k \sigma_{kl} \ , \tag{5}$$

where σ_{kl} takes the values 1 or 0 if the site of coordinates (k,l) is occupied or empty, respectively. The summation over occupied sites in a row is now replaced by summation over all sites multiplied by the fractional occupation of the row [n_k; for its definition see Eq. (15)], hence

$$E_i^1 = -(1/a^3) \sum_{k=1}^{L_T} \sum_{l=-L/2}^{L/2} n_k p_k [(k-i)^2 + l^2]^{-3/2} \ . \tag{6}$$

The introduced assumption, which implies that the dipoles of each row are on average randomly distributed, has been checked by means of a Monte Carlo simulation on a two-dimensional lattice[10] and we expect that it would also hold for the present case. Also, the curves n_k versus k are the concentration profiles which will be calculated in Sec. III. For large values of L, Eq. (6) becomes

$$E_i^1 = -(1/a^3) \sum_{k=1}^{L_T} n_k A_{k,i} \tag{7a}$$

with

$$A_{k,i} = \sum_{l=-\infty}^{+\infty} [(k-i)^2 + l^2]^{-3/2} = A_{|k-i|} \ , \tag{7b}$$

that is, $A_{k,i}$ depends on $|k-i|$ and in summation (7a) one should remember that $l \neq 0$ for $|k-i| = 0$.

The depolarization field due to the images of the adsorbed dipoles can be written as

$$E_i^2 = \sum_{k=1}^{L_T} \sum_{l=-\infty}^{+\infty} \frac{3p_{kl}(2\beta)^2}{a^5[(k-i)^2 + l^2 + (2\beta/a)^2]^{5/2}} - \frac{p_{kl}}{a^3[(k-i)^2 + l^2 + (2\beta/a)^2]^{3/2}} \tag{8}$$

with the restriction $(k,l) \neq (i,0)$, where β is the distance between the point dipole and the image plane. Under the same assumptions used to obtain Eqs. (7a) and (7b), one has that Eq. (8) can be written as

$$E_i^2 = (1/a^3) \sum_{k=1}^{L_T} n_k p_k (B_{ki} - C_{ki}) \tag{9a}$$

with

$$B_{ki} = \sum_{l=-\infty}^{+\infty} \frac{3(2\beta/a)^2}{[(k-i)^2 + l^2 + (2\beta/a)^2]^{5/2}} = B_{|k-i|} \tag{9b}$$

and

$$C_{ki} = \sum_{l=-\infty}^{+\infty} [(k-i)^2 + l^2 + (2\beta/a)^2]^{-3/2} = C_{|k-i|} \ . \tag{9c}$$

Replacing the depolarization fields given by Eqs. (7) and (9) in Eq. (2) one has

$$p_i = p_i^0 - (\alpha/a^3) \sum_{k=1}^{L_T} n_k p_k (A_{|k-i|} - B_{|k-i|} + C_{|k-i|}) \tag{10}$$

with $1 \leq i \leq L_T$. Regrouping the terms in p_i one obtains a system of L_T equations with L_T unknowns, i.e., the dipole moments p_i.

Now the system of Eq. (10) has to be solved for various coverages, and Eq. (1) for the adsorbate-induced work-function changes on stepped surfaces ($\Delta\phi_s$) can be generalized to account for the depolarization interaction as follows:

$$\Delta\phi_s = -4\pi(1/a^2 L_T) \sum_{i=1}^{L_T} n_i p_i \ . \tag{11}$$

A similar formalism has also been employed to explain experimental results on both work-function changes upon coadsorption[12] and adsorbate clustering.[11] The treatment developed above also allows us to calculate the dipolar potential energy ε_i of a dipole at the ith row which is given by

$$\varepsilon_i = -p_i(E_i^1 + E_i^2) \ . \tag{12}$$

III. THE CONCENTRATION PROFILE

Let us now briefly discuss the Monte Carlo procedure employed to obtain the concentration profiles.[15] The particles are assumed to be adsorbed on a two-dimensional square lattice of size $L \times L_T$ ($L = 153$ and $L_T \leq 51$). Periodic boundary conditions along the direction parallel to the step have also been used in order to avoid edge effects. Double occupancy of lattice sites is forbidden. Each particle is bound to the surface with a binding energy U_0 and each pair of particles in nearest-neighbor sites contributes an amount W to the potential energy. Also, each particle in the ith row experiences an additional potential energy $V(i)$ due to the step placed at $i = 0$, given by

$$V(i) = V_0 W / i^3, \quad 1 \leq i \leq L_T \tag{13}$$

where the strength of the potential V_0 is a dimensionless parameter which allows us to express $V(i)$ in the W energy scale. Under the above assumptions, the Hamiltonian (H) of the system is

$$H = -U_0 \sum_{i,j} \sigma_{ij} - W \sum_{\langle ij, i'j' \rangle} \sigma_{ij}\sigma_{i'j'} - \sum_{i,j} V(i)\sigma_{ij} \ , \tag{14}$$

where $\langle\ \rangle$ denotes a nearest-neighbor pair of sites. At the first step of the Monte Carlo simulations, the lattice sites are filled in with probability Θ (Θ is the surface coverage which remains constant through all the procedure). Figure 1(a) shows an example of an initial configuration on a lattice size $L = 121$ by $L_T = 21$ with $\Theta = 0.40$. Since the adparticles are randomly distributed only small clusters can be observed at low coverages ($\Theta < 0.5$). After deposition at random, the diffusion of adparticles is simulated. At each time step the probability that a randomly chosen particle at the site h jumps to a randomly chosen q nearest-neighbor empty site is $\exp(-\delta H/kT)$ if $\delta H > 0$, or 1 otherwise; where k is the Boltzmann constant, T the temperature, and δH is the energy change due to the movement of one particle from h to q. After a large number of jumps, the equilibrium configuration is obtained (for more detail see Ref. 15). Figures 1(b) and 1(c) show

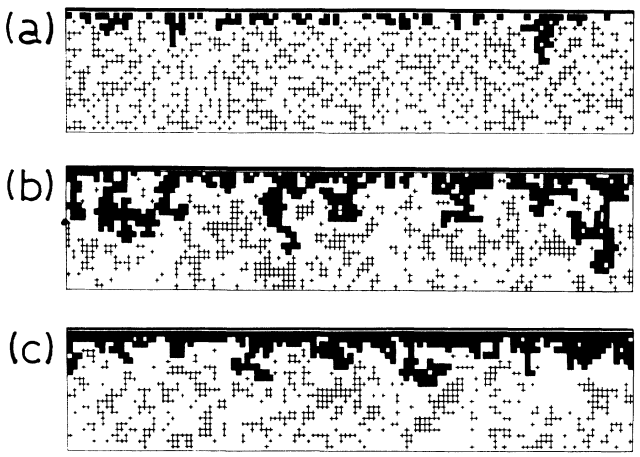

FIG. 1. Snapshots of the adsorbate distribution on a terrace of stepped surface, as obtained from Monte Carlo simulations. ■, particles and clusters in contact with the step indicated by the heavy line at the upper part of the respective figure. +, the remaining adsorbed on the terrace. $\Theta = 0.40$, $L = 151$, and $L_T = 41$. Note the periodic boundary conditions in the direction parallel to the step. (a) Configuration of particles deposited at random. (b) and (c) Snapshots of equilibrium configurations obtained assuming $W/kT = 1.0$ and $V_0 = 1$ and 5, respectively.

snapshots obtained, at the equilibrium regime, assuming $W/kT = 1$ and different values of the potential strength $V_0 = 1$ and 5. The strong attractive interaction between the adparticles leads to the formation, in all cases, of bigger and more compact clusters than for random adsorption [Fig. 1(a)]. Moreover, in the competition between particle nucleation at clusters on terrace sites (crosses) and clusters attached to the step (solid squares), the latter becomes clearly dominant when the step-adatom interaction is increased (that is, on going from the upper to the lower part of Fig. 1). A great variety of adsorbate-adsorbent systems exhibit selective growth of adparticles at step sites. In fact, since the early experiment of Basset,[17] this preferential growth is the basis of the well-known "surface decoration technique," which allows the detection of surface defects, such as steps, dislocations, etc. (See, for example, Ref. 18.) The concentration profile (n_i) of adparticles in the direction perpendicular to the step placed at $i = 0$ is obtained by using

$$n_i = (1/L) \sum_{j=1}^{L} \sigma_{ij}, \quad 1 \leq i \leq L_T \ . \tag{15}$$

The values of n_i to be replaced in Eq. (11) for the evaluation of the WFC's are obtained by averaging over 100 equilibrium configurations (similar to those shown in Fig. 1) for each value of Θ, L_T, W/kT, and V_0.

In the Monte Carlo simulations the dipolar potential energy ε_i can be neglected as compared with W and this approximation becomes better when increasing the polarizability (see also the last part of Sec. IV). For more details of the Monte Carlo procedure the reader is referred to our previous work.[15]

IV. RESULTS

For the sake of comparison we have considered it useful to present only those results obtained keeping fixed some parameters of the model. Therefore in all cases discussed further on, one has $L_T=11$ and $a=5$ Å. Available results show that β is of about half the substratum-adatom bond length,[9-11] i.e., $2\beta \simeq R_s + a/2$ where R_s is the atomic radii of the substratum. In the following we assume $2\beta=a$, i.e., $R_s \simeq a/2$, while in principle β is an adjustable parameter of the model. Furthermore, we have used $p_s=p_1^0=0.9$ D for isolated dipoles at step sites and $p_T=p_i^0=0.3$ D (with $2 \leq i \leq L_T$) for isolated dipoles at terrace sites. The values of p_s and p_T have been selected considering the reported difference between the magnitude of the dipole moments for particles adsorbed at step and on terrace sites as it follows from WFC measurements on well-characterized stepped surfaces[19,20] (see also Table I in Ref. 15).

Figure 2 shows the WFC's versus Θ as evaluated using Eq. (11) for stepped surfaces assuming $V_0=5$, $\alpha=0$, and different values of W/kT. The slope of the straight line obtained for the high-temperature behavior ($W/kT=0$, i.e., random adsorption) defines an effective dipole moment $p_{\text{eff}}=p_T+(p_s-p_T)/L_T$ (Ref. 15) with $p_{\text{eff}}=0.35$ D. In this particular case, measurements of the WFC's are not sensitive to the presence of surface steps since the same straight line should be obtained by using a flat surface and assuming p_{eff} as the dipole moment of the adparticles. Lowering the temperature of the sample, the Monte Carlo simulations show (see Fig. 1) that the particles are preferentially adsorbed close to step sites in agreement with most of the available experimental data. This behavior which is introduced into Eq. (11) through the concentration profiles is clearly evidenced in the calculated WFC's as it is shown in Fig. 2 for $W/kT=0.5$ and $W/kT=1.0$. Precisely, the preferential adsorption at step sites, with higher dipole moment, causes the work function to change more than for the previous case of random adsorption. For $W/kT=1$ and strong enough step-adatom interaction ($V_0=5$), the plot of $\Delta\phi_s$ versus Θ has two well-defined regions of linear variation which allow us to recover the input values of p_s and p_T. This behavior is in excellent agreement with available experimental data for the systems Xe/Ru(0001) (Ref. 19) and Xe/Pd [8(100)×(110)],[20] as it has previously been analyzed in detail,[15] therefore it has been briefly discussed here for the sake of comparison with the results presented further on.

Figure 3 shows the dependence of both the concentration profile and the total electrical depolarization field E_i, given by Eqs. (3), (7), and (9) on the distance perpendicular to the direction of the step, for $\Theta=0.4$, $W/kT=1$, and the same parameters as those used in Fig. 2. The abrupt decrease of the concentration profile upon increasing the distance to the step indicates the preferential nucleation of adparticles close to the step as has just been mentioned. For $\alpha=0$, and due to both the higher dipole moment of the adatoms at step sites comparing with those on terrace sites and the preferential growth close to the step, $|E_i|$ also abruptly decreases upon increasing the distance to the step. In fact, for the example shown in Fig. 3 the field at the first two rows ($i=1,2$) close to the step is roughly 1 order of magnitude higher than the field at the last ($i=L_T$) row. This situation can no longer remain for $\alpha>0$, but in order to analyze this case it is convenient to make some remarks about the polarizability. Since in the system of equations which gives the dipole moments [Eq. (10)] the polarizability always appears combined with the nearest-neighbor distance in the form

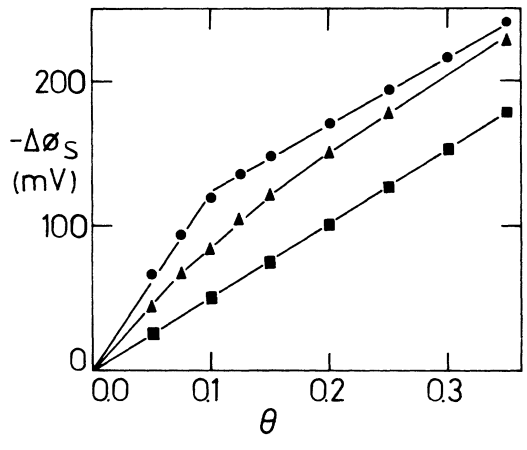

FIG. 2. Plot of $\Delta\phi_s$ vs Θ as calculated with Eq. (11) for adsorption on stepped surfaces. $L_T=11$, $a=5$ Å, $p_1=0.9$ D, $p_i=0.3$ D ($2 \leq i \leq L_T$), and $\alpha=0$. (a) ■, random adsorption ($W/kT=0$). From the slope of the straight line an effective dipole moment of $p_{\text{eff}}=0.35$ D has been obtained using Eq. (1). (b) ▲, $V_0=5$, $W/kT=0.5$. (c) ●, $V_0=5$, $W/kT=1$. From the slope of the low- (high-) coverage-regime straight line a step (terrace) effective dipole moment of $p_s=0.3$ D ($p_T=0.87$ D) has been obtained.

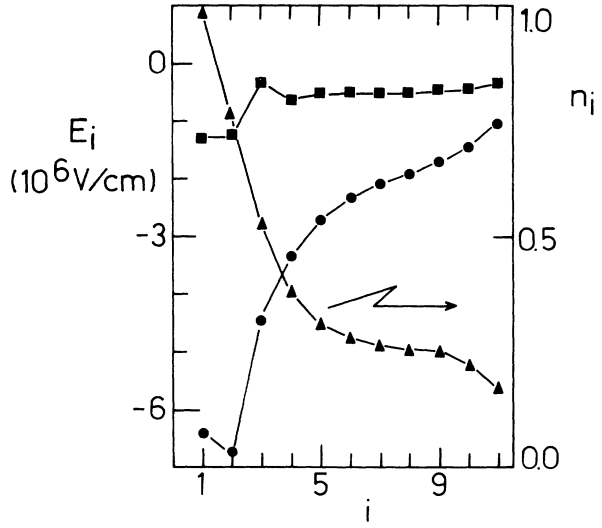

FIG. 3. The concentration profiles (n_i, right-hand axis) vs the distance to the step in units of the nearest-neighbor distance a; ▲, $L_T=11$, $V_0=5$, $W/kT=1.0$, $\Theta=0.4$. Plot of the depolarization field (E_i, left-hand axis) vs the distance to the step. ●, $\alpha_0=0.0$; ■, $\alpha_0=1.0$. The lines have been drawn to guide the eyes.

α/a^3, it is useful to define a dimensionless polarizability by $\alpha_0=\alpha/a^3$. The relevant range of α_0 can be determined using typical values of α and a. For example, for free-space metal atoms such as Ag, Au, Pt, Ir, and W, α increases from 9.2 to 16.8 Å^3,[21] while for these metals a is roughly about 2.8 Å, which gives $0.4\lesssim\alpha_0\lesssim 0.8$. Also, for Xe one has $\alpha=4.01$ Å^3 (Ref. 21) and $a=4.5$ Å,[20] that is $\alpha_0=4.4\times10^{-2}$, which is consistent with the fact that Xe-induced WFC's are well interpreted by Eq. (11) with $\alpha=\alpha_0=0$ (see Fig. 2). It should also be mentioned that a fourfold adsorption-induced enhancement of the polarizability has been reported for Ni on Ni(111) (Ref. 2) ($\alpha_f=7$ Å^3 and $\alpha_a=24$ Å^3 for the free and the adsorbed Ni atom, respectively). Therefore, in the present work we have analyzed the range $0\le\alpha_0\le 1.0$ which involves most of the cases of interest. Adsorption systems with higher polarizabilities such as alkali-metal atoms on transition-metal surfaces lie out of the studied range of α_0, but also the concentration profiles derived through the Monte Carlo simulations are not useful for these systems since the structure of the adlayer is determined by the dipolar repulsion[4,13] rather than by the energies considered in the Hamiltonian of Eq. (14).

For $\alpha_0>0$ the depolarization field causes the reduction of the dipole moments with the consequent reduction of the depolarization field in a self-consistent manner. This behavior is evidenced in Fig. 3 for $\alpha_0=1.0$, where E_i smoothly depends on the distance to the step. An additional effect, due to the strong depolarization field close to the step, is the change in the direction of the electrical dipoles in some rows, as is discussed further on.

Figure 4 shows the influence of the polarizability on the WFC's for random adsorption on stepped surfaces ($W/kT=0$). The straight line for $\alpha_0=0$ has also been included for the sake of comparison with Fig. 2. For $\alpha_0>0$ deviations from the straight-line behavior are a consequence of the dipolar interaction which causes the dipole moments of all the rows to decrease with respect to the value for isolated adsorbed particles. Obviously for a fixed coverage and $\alpha_0>0$ all the calculated WFC's are of less magnitude than for the case $\alpha_0=0$. Nevertheless, bent curves with a marked tendency for saturation at high coverage, as those shown in Fig. 4 for $\alpha_0\gtrsim 0.5$, do not give enough information by themselves to infer some of the properties of the system under study, such as surface distribution of the adsorbate, polarizability, etc. This statement can be easily understood after inspection of Fig. 5, which shows the dependence of the WFC's upon coverage for the case of preferential nucleation at step sites with $V_0=5$, $W/kT=1$, and different values of α_0. The case $\alpha_0=0$, with the typical two-straight-line behavior, has also been included for the sake of comparison with Fig. 2. For $\alpha_0>0.25$, the knee observed with $\alpha_0=0$ can no longer be distinguished and after a visual inspection the curves are similar to those obtained for both random adsorption (Fig. 4 with $\alpha_0\neq0$) and interactive adsorption at the intermediate-temperature regime (Fig. 2 with $\alpha_0=0$ and $W/kT=0.5$).

Summing up, let us stress that the results presented in Figs. 2, 4, and 5 clearly point out the limitations of the WFC measurements performed at a single temperature. The situation may be even worse in the case of WFC's upon adsorption on polycrystalline samples due to the preferential nucleation of the adsorbate not only at step sites but also at grain boundaries, intercrystalline gaps, and other surface defects. Also, one may expect that particles adsorbed at these sites should have different dipole moments. For $\alpha_0\gtrsim 0.2$, careful measurements on stepped surfaces covering a width range of adsorption temperatures should be compared with results from single-crystal flat surfaces, in order to allow an independent determination of p_T from the initial slope of the WFC versus Θ curves.

Another interesting prediction of the model is that, due to the depolarization electrical field and depending on α_0, the dipole moments of the particles adsorbed on some rows of a stepped surface could have the opposite direction from isolated adparticles on the same rows. In fact,

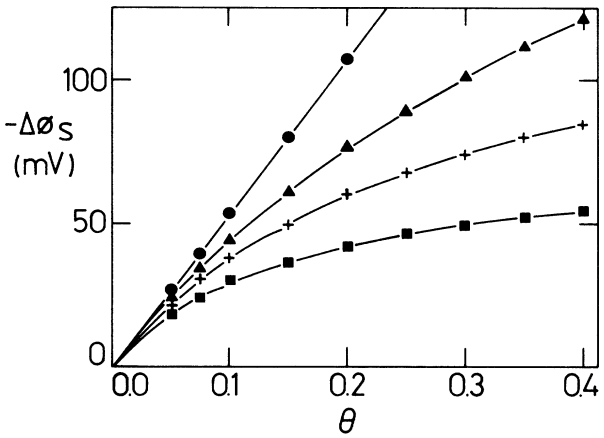

FIG. 4. Plot of $\Delta\phi_s$ vs Θ as calculated with Eq. (11) for random adsorption ($W/kT=0$) on stepped surfaces. $L_T=11$, $a=5$ Å, $p_1=0.9$ D, $p_i=0.3$ D ($2\le i\le L_T$), and different values of α_0. ●, $\alpha_0=0.0$; ▲, $\alpha_0=0.25$; +, $\alpha_0=0.50$; ■, $\alpha_0=1.0$.

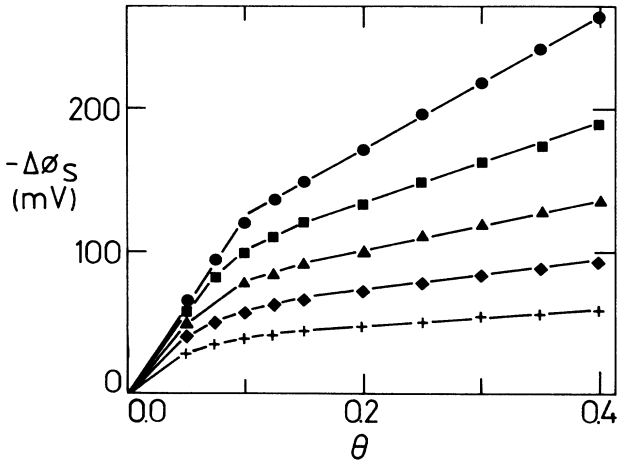

FIG. 5. Plot of $\Delta\phi_s$ vs Θ as calculated with Eq. (11) for adsorption on stepped surfaces. $L_T=11$, $a=5$ Å, $p_1=0.9$ D, $p_i=0.3$ D ($2\le i\le L_T$), $V_0=5$, $W/kT=1$, and different values of α_0. ●, $\alpha_0=0.0$; ■, $\alpha_0=0.10$; ▲, $\alpha_0=0.25$; ♦, $\alpha_0=0.50$; +, $\alpha_0=1.0$.

Fig. 6 shows the dependence of p_i $(1 \leq i \leq 3)$ versus α_0 for $\Theta = 0.10$ and two cases: random adsorption ($W/kT = 0.0$) and preferential nucleation at step sites ($V_0 = 5$ and $W/kT = 1.0$). At this low coverage and for $W/kT = 0.0$, the dipole moments of all the rows slightly decrease with respect to the values of the isolated particles. On the other hand, the preferential adsorption close to the step causes the depolarization field to increase in this region, and consequently the dipole moment appreciably decreases for $i = 1$. The influence of the depolarization effect is more dramatic for $i = 2$ since the dipole moment changes its original direction for $\alpha_0 > \alpha_{0i}^*$, where α_{0i}^* is the value of the polarizability where the dipole moment at the ith row is zero. In Fig. 6 $\alpha_{02}^* \simeq 0.25$. At low coverages, $\Theta = 0.10$ in the example of Fig. 6, only minor differences between random and preferential adsorption can be appreciated for $i > 3$.

It is also interesting to study how this depolarization-induced inversion of the dipole moment is propagated through all the rows at higher coverages. Figure 7 shows the variation of p_i $(1 \leq i \leq 6)$ versus α_0 for $\Theta = 1.0$. Note that the assumptions made for the evaluation of the depolarization fields in Sec. II, concerning both the random distribution of the particles along the rows and the magnitude of the dipole moments, are strictly valid for $\Theta = 1.0$, while on the other hand, the assumption of noninteraction between dipoles adsorbed at different terraces becomes weaker. At this coverage the direction of the dipole moment is reversed in three rows $i = 2$, 4, and 6 with $\alpha_{01}^* \cong 0.21$, $\alpha_{04}^* \cong 0.67$, and $\alpha_{06}^* \cong 0.90$. Note that the change in the direction of the dipole moments of rows 2 and 4 compensates and even reverses the decreasing trend of the dipole moments of the neighboring rows ($i = 1$, 3, and 5). In Fig. 7(a) (first row), we have also shown the dependence of p_1 versus α_0 assuming full adsorption on the first row only, in order to show the compensation of the decreasing trend of p_1, observed for $\Theta = 1$, due to the depolarization effects of the other rows. The depolarization-induced inversion of the dipole moment should be clearly evidenced in measurements of the WFC's caused by adsorption on stepped surfaces in a "row-by-row" mode, i.e., a one-dimensional analog of the well-known "layer-by-layer" Frank–van der Merwe[22]

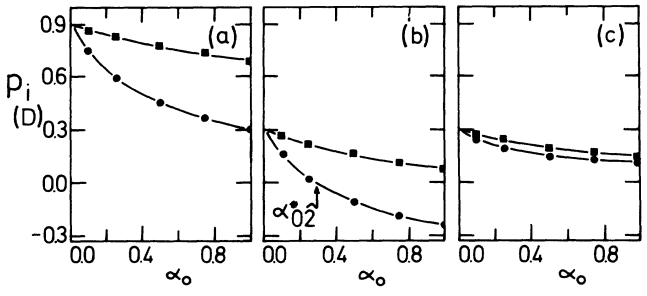

FIG. 6. Dependence of the dipole moments of the rows close to the step on the polarizability for adsorption on stepped surfaces. $L_T = 11$, $a = 5$ Å, $p_1 = 0.9$ D, $p_i = 0.3$ D $(2 \leq i \leq L_T)$, and $\Theta = 0.10$. ■, $W/kT = 0.0$; ●, $V_0 = 5$ and $W/kT = 1.0$. (a) First row, (b) second row (the arrow indicates the polarizability at $p_2 = 0$), and (c) third row.

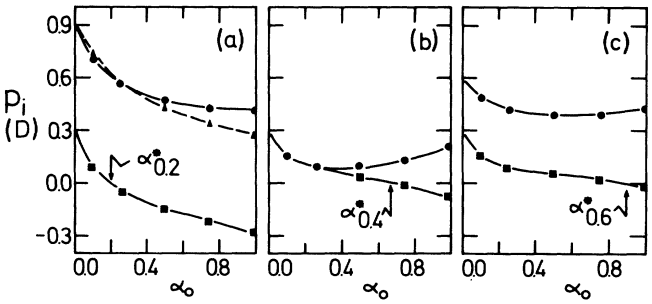

FIG. 7. Dependence of the dipole moments of the different rows on the polarizability for adsorption on stepped surfaces. $L_T = 11$, $a = 5$ Å, $p_1 = 0.9$ D, $p_i = 0.3$ D $(2 \leq i \leq L_T)$, and $\Theta = 1.0$. (a) ●, first row; ■, second row. The dashed line (▲) shows the dependence of p_1 vs α_0 assuming row-by-row growth up to the completion of the first row only. (b) ●, third row; ■, fourth row. (c) ●, fifth row; ■, sixth row. The arrows indicate the polarizability at $p_i = 0$ ($i = 2$, 4, and 6).

growth mechanism in two-dimensional substrate. Figure 8 shows the WFC's versus Θ for a row by row growth assuming $\alpha_0 = 1$. Also the WFC's for random and preferential adsorption ($V_0 = 5$, $W/kT = 1.0$) for $\alpha_0 = 1.0$ have been included for the sake of comparison. At low coverage, $\Theta \lesssim 0.1$, the curves for the row-by-row mode and preferential adsorption at step sites are overlapped, as expected due to the growth at step sites in both cases. Nevertheless, the depolarization-induced dipole inversion causes an oscillatory behavior of the work function, substantially different from the smooth variations observed for random and strong step-adatom interactive adsorption. Maxima and minima on the WFC versus Θ curve are observed at the completion of odd and even rows, respectively, in agreement with the results shown in Fig. 7. A similar behavior to that shown in Fig. 8 for the row-by-row mode has been reported for the WFC's upon hydrogen adsorption on Pt stepped surfaces where the di-

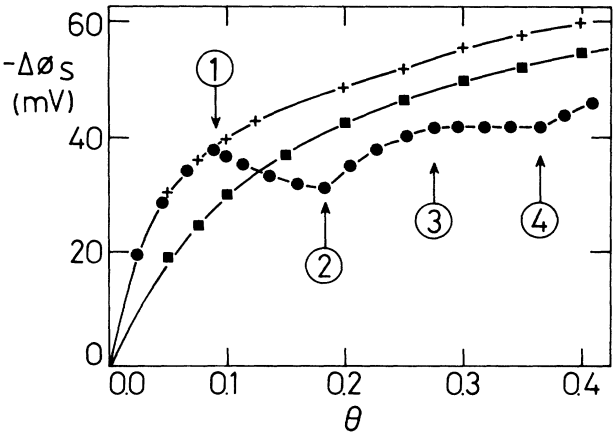

FIG. 8. Plot of $\Delta\phi_s$ vs Θ as calculated with Eq. (11) for adsorption on stepped surfaces. $L_T = 11$, $a = 5$ Å, $p_1 = 0.9$ D, $p_i = 0.3$ D $(2 \leq i \leq L_T)$, and $\alpha_0 = 1.0$. +, $V_0 = 5$ and $W/kT = 1.0$; ■, random adsorption ($W/kT = 0$); ●, row-by-row growth mode. The arrows indicate the completion of the successive rows.

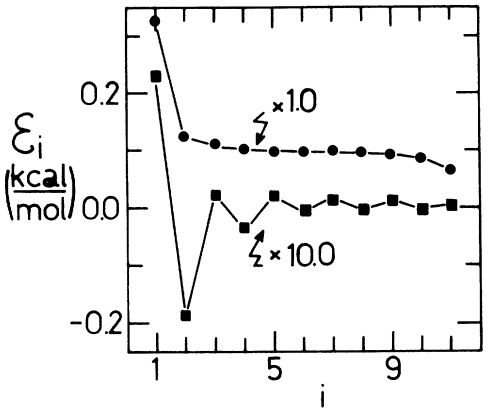

FIG. 9. The dipolar interaction energy (ε_i) vs the distance to the step in units of the nearest-neighbor distance a. $L_T=11$, $\Theta=1.0$, $a=5$ Å, $p_1=0.9$ D, and $p_i=0.3$ D ($2\leq i\leq L_T$). ●, $\alpha_0=0.0$; ■, $\alpha_0=1.0$ (note the enlargement of the scale). The lines have been drawn to guide the eye.

pole moment of the hydrogen atoms at the first row is negative while for the second one it is positive.[16,23] Nevertheless, the origin of this particular behavior remains without an unambiguous explanation.

Another interesting consequence of the depolarization-induced inversion of the dipole moment concerns the dipolar interaction energy [ε_i, see Eq. (12)] on the adlayer. Figure 9 shows the dependence of ε_i on the distance perpendicular to the step for $\Theta=1.0$. For $\alpha_0=0$ one has $p_1^0=0.9$ D and $p_i^0=0.3$ D ($2\leq i\leq 11$) and therefore the interaction energy between dipoles is repulsive ($\varepsilon_i>0$). Also, as expected, $\varepsilon_1>\varepsilon_i$ ($2\leq i\leq 11$). When increasing the polarizability one passes through the successive values of α_{0i}^* and therefore the depolarization-induced inversion of the dipole moments begins to play a role. In fact, for $\alpha_0=1.0$ the interaction energy at each particular row not only decreases, roughly 1 order of magnitude, but also all the rows labeled with an even index experience an attractive dipolar interaction.

It should be noticed that the concentration profiles obtained through the Monte Carlo simulations can be used to evaluate the WFC's with the aid of Eq. (11) when the dipolar interaction is negligible with respect to the adatom-step and adatom-adatom interaction energies which appear in the Hamiltonian of Eq. (14). This assumption does not represent a severe restriction for the results discussed above. In fact, for $a=5$ Å, $p_1^0=0.9$ D, $p_1^0>p_i^0$ ($i>1$), and $\alpha_0=0$, the strongest repulsion energy between nearest-neighbor dipoles at the first row ($\cong 0.1$ kcal/mol) is roughly one-half that of the bulk nearest-neighbor interaction W_b between Xe atoms.[24] The approximation becomes improved for adsorbates with interacting energies W_b larger than for noble gases and for $\alpha_0>0$, as evidenced by the diminution of roughly 1 order of magnitude in ε_i shown in Fig. 9.

V. CONCLUSIONS

The dipolar interaction between particles adsorbed on stepped surfaces is studied and discusses. From the results obtained we conclude the following.

(1) The proposed generalization of the Helmholtz equation to account for the dipolar interaction in the adlayer on stepped surfaces [Eq. (11)] in connection with concentration profiles obtained through Monte Carlo simulations allows us to study the influence on the polarizability and the temperature on the adsorbate-induced WFC's on stepped surfaces.

(2) The well-defined two-straight-line behavior of the measured Xe-induced WFC's versus coverage on stepped surfaces is a consequence of the different dipole moment of the adatoms at step and on terrace sites, the preferential nucleation of the adsorbate close to the step and the negligible depolarization interaction between the adatoms ($\alpha_0\cong 4.4\times 10^{-2}$).

(3) The adsorbate-induced WFC's on stepped surfaces depend on the surface distribution and the polarizability of the adparticles, the former being a function of the adatom-adatom and step-adatom interactions (W/kT and V_0W/kT, respectively). Since the WFC versus coverage curves obtained for some different values of α_0, W/kT, and V_0 are quite similar, it becomes difficult to properly separate the relevant influence in measurements performed at constant temperature on stepped surfaces. In light of this result we expect that WFC measurements on polycrystalline surfaces can only be described in a qualitative manner.

(4) Dipolar interaction between adparticles would cause the so called depolarization-induced dipole inversion. This phenomenon consists in the change of the direction of the dipole moments in some rows with respect to the dipole moments of the respective isolated particles in the same rows. It will be expected that this behavior could be evidenced in measurements of the WFC at low adsorption temperature and for the case of very strong adatom step attractive interaction, i.e., the so called row-by-row growth mode.

(5) Dipolar effects for $\alpha_0>0$ cause both the depolarization field and the repulsive dipolar interaction energy to decrease with respect to the value for $\alpha_0=0$. In particular, when the increment of α_0 causes the depolarization-induced dipolar inversion, the dipolar interacting energy becomes attractive in some rows.

ACKNOWLEDGMENT

This work was financially supported by the Consejo Nacional de Investigaciones Científicas y Técnicas (CONICET), Argentina.

*Present address: Institut für Physik, Universität Mainz, Postfach 3980 D-6500 Mainz 1, Federal Republic of Germany.

[1]J. Hölzl and F. K. Schulte, in *Work Function of Metals,* Vol. 85 of *Springer Tracts in Modern Physics,* edited by G. Höhler (Springer-Verlag, Berlin, 1979).

[2]J. Hölzl, G. Porsch, and P. Schrammen, Surf. Sci. **97**, 529 (1980).

[3]R. A. de Paola, J. Hrbek, and F. M. Hoffmann, J. Chem. Phys. **82**, 2484 (1985).

[4]R. L. Gerlach and T. N. Rhodin, Surf. Sci. **19**, 403 (1970).

[5]S. B. Lee, M. Weiss, and G. Ertl. Surf. Sci. **108**, 357 (1981).

[6]J. E. Crowell, E. L. Garfunkel, and G. A. Somorjai, Surf. Sci. **121**, 303 (1982).

[7]H. Pfnür, D. Menzel, F. M. Hoffmann, A. Ortega, and A. M. Bradshaw, Surf. Sci. **93**, 431 (1980).

[8]B. N. J. Persson and A. Liebsch, Surf. Sci. **110**, 356 (1981).

[9]J. R. Macdonald and C. A. Barlow, J. Chem. Phys. **39**, 412 (1963); **44**, 202 (1966); Surf. Sci. **4**, 381 (1966).

[10]J. M. Heras and E. V. Albano, Z. Phys. Chem. **126**, 57 (1981).

[11]J. M. Heras, E. V. Albano, P. Schrammen, M. Mann, and J. Hölzl, Surf. Sci. **129**, 137 (1983).

[12]E. V. Albano, Appl. Surf. Sci. **14**, 183 (1982).

[13]E. V. Albano, J. Chem. Phys. **85**, 1044 (1986).

[14]N. D. Lang, Phys. Rev. B **4**, 4234 (1971).

[15]E. V. Albano and H. O. Mártin, Phys. Rev. B **35**, 7820 (1987).

[16]H. Wagner, in *Physical and Chemical Properties of Stepped Surfaces,* Vol. 85 of *Springer Tracts in Modern Physics,* edited by G. Höhler (Springer-Verlag, Berlin, 1979).

[17]G. A. Bassett, Philos. Mag. **3**, 1042 (1958).

[18]J. G. Allpress and J. V. Sanders, J. Catal. **3**, 528 (1964).

[19]K. Wandelt, J. Hulse, and J. Kuppers, Surf. Sci. **104**, 212 (1981).

[20]R. Miranda, S. Daiser, K. Wandelt, and G. Ertl, Surf. Sci. **131**, 61 (1983).

[21]R. Forbes, Surf. Sci. **64**, 367 (1977).

[22]G. E. Rhead, J. Vac. Sci. Technol. **13**, 603 (1976).

[23]G. Ertl, in *The Nature of the Surface Chemical Bond,* edited by T. N. Rhodin and G. Ertl (North-Holland, Amsterdam, 1979), p. 345.

[24]R. Miranda, E. V. Albano, S. Daiser, K. Wandelt, and G. Ertl, J. Chem. Phys. **80**, 2931 (1984).